UFSM

CIÊNCIA e NATURA

ISSN 2179-460X

OPEN ACCESS

Ci. e Nat., Santa Maria, v. 47, spe. 1, e89848, 2025• https://doi.org/10.5902/2179460X89848
Submitted: 11/20/24 • Approved: 11/26/24 • Published: 01/15/25

IV Jornada de Matematica e Matematica aplicada UFSM

On an agent-based SIR model for multi-populations

Um modelo do tipo SIR baseado em agentes para múltiplas populações

Lara Beatriz Rocha Vieira [I], **Fabiana Travessini De Cezaro** [I], **Adriano De Cezaro** [I]

[I]Universidade do Rio Grande, RS, Brazil

ABSTRACT

In this paper, we investigate the impact of epidemic spread in a SIR type model with saturation between multiple interacting populations. The model is derived from an average threshold that considers multiple agents. Theoretical analysis confirms the model's well-posedness, indicating that it possesses a unique solution that varies continuously on the basis of the initial conditions and parameters. Additionally, we conduct numerical simulations for a scenario involving two circulating strains, where we also explore the scenario in which the disease mutates upon transmission, leading to increased transmissibility. A comparison between the dynamics of the SIR model with and without saturation reveals that saturation results in a milder disease dynamics.

Keywords: Saturated SIR model; Multi-Population dynamics; Diseases transmission; Predictions

RESUMO

Neste artigo, investigamos o impacto da propagação epidêmica em um modelo do tipo SIR com saturação entre múltiplas populações em interação. O modelo é derivado de um limite médio que considera múltiplos agentes. A análise teórica confirma a boa colocação do modelo, indicando que ele possui uma solução única que depende continuamente das condições iniciais e parâmetros. Além disso, realizamos simulações numéricas para um cenário envolvendo duas cepas circulantes, onde também exploramos o cenário em que a doença sofre mutação durante a transmissão, levando ao aumento da transmissibilidade. Uma comparação entre a dinâmica do modelo SIR com e sem saturação revela que a saturação resulta em uma dinâmica mais branda da doença.

Palavras-chave: SIR saturado; Multiplas populações; Transmissão de doenças; Previsões

1 INTRODUCTION

The occurrence of significant events that bring about profound changes in human life globally triggers an ongoing quest for solutions and methods to anticipate similar events in the future, as well as strategies for prevention Dhaoui et al. (2022). Unsurprisingly, the global outbreak of the coronavirus pandemic sparked a worldwide competition among researchers to develop epidemiological models that can elucidate the patterns of contagion. This rush was so intense that conducting a comprehensive review of recent literature became nearly impracticable Dhaoui et al. (2022). Broadly speaking, the suggested models encompass SIR-type compartmental models Allen (2007); Hethcote (2000); Kermack & Mckendrick (1927), statistical models Allen (2007), agent-based models Kolokolnikov & Iron (2021), models that depict individuals interconnected on a network Lazo & De Cezaro (2021); Marques et al. (2022,2); Maurmann et al. (2023), and others.

The core of most mathematical models in epidemiology is based on SIR-type compartmental models Allen (2007); Hethcote (2000); Lazo & De Cezaro (2021); Marques et al. (2022,2); Maurmann et al. (2023). In these models, each of the n (potentially different) populations is segmented into compartments, labeled as $S_i(t)$, $I_i(t)$, $R_i(t)$, which indicate the proportion of the population i, for $i = 1, \cdots, n$, that are susceptible, infected, and recovered at time $t \geq 0$, respectively. Assuming that the disease spreads when a person from compartment $S_i(t)$ encounters someone from compartment $I_j(t)$, where the likelihood of this interaction is proportional to $S_i(t)I_j(t)$ with an infection rate denoted as β_{ij}, the conservation of mass principle implies that the dynamics of the model should be described as

$$\begin{aligned} S_i'(t) &= -S_i(t)\left(\sum_{j=1}^{n}\frac{\beta_{ij}}{N_j}I_j(t)\right), \\ I_i'(t) &= S_i(t)\left(\sum_{j=1}^{n}\frac{\beta_{ij}}{N_j}I_j(t)\right) - \gamma_i I_i(t), \\ R_i'(t) &= \gamma_i I_i(t), \end{aligned} \tag{1}$$

where $N_i = S_i(t) + I_i(t) + R_i(t)$, for $i = 1, \cdots, n$, represents the total population, which remains consistent, and γ_i denotes the recovery rate. The model in Equation (1) is an

SIR-type model designed for multiple populations that have interactions with each other, as discussed in Lazo & De Cezaro (2021); Marques et al. (2022,2); Maurmann et al. (2023) and related literature. In Lazo & De Cezaro (2021); Marques et al. (2022,2), the authors show that the multi-population SIR model (1) presents a plateau-like behavior in the total infected population as n is large and the population density is decreasing. This phenomenon is not observed in the classical SIR models without control strategies, e.g. Allen (2007); Hethcote (2000), since the population is considered homogeneous.

If we take into account a crucial aspect of dynamics where Λ_i represents the rate at which new individuals are recruited due to birth or immigration into the susceptible population, and m_i denotes the fixed death rate, then the model described by Equation (1) can be expressed as

$$\begin{aligned} S_i'(t) &= \Lambda_i - S_i(t)\left(\sum_{j=1}^{n}\frac{\beta_{ij}}{N_j}I_j(t)\right) - m_i S_i(t)\,, \\ I_i'(t) &= S_i(t)\left(\sum_{j=1}^{n}\frac{\beta_{ij}}{N_j}I_j(t)\right) - (\gamma_i + m_i)I_i(t)\,, \\ R_i'(t) &= \gamma_i I_i(t) - m_i R_i(t)\,. \end{aligned} \tag{2}$$

The model (1) or model (2) needs to be taken into account along with the subsequent initial conditions

$$S_i(0) \geq 0\,, \quad I_i(0) \geq 0\,, \quad R_i(0) \geq 0\,. \tag{3}$$

The SIR model in (1) or (2) assumes that the contacts between an infectious I_j and susceptible individual S_i, for $i, j \in \{1, \cdots, n\}$, is given by the law of mass action in chemistry, which results in the susceptible person becoming infected due to the random "collision" (with zero distance) between infectious and susceptible individual, e.g. Allen (2007). However, it is well known that many diseases are transmitted by airbone particle, for example Influenza, Tuberculosis, Measles, Covid-19 among others, e.g. Kutter et al. (2018), where susceptible individuals can be infected without a direct contact with an infected individual. In other words, a susceptible individual can be infected even when remains in a distance (not null) of infected individual, see Kolokolnikov & Iron (2021) for some motivations regards the Covid-19 data and references therein.

In this paper, we introduce a modification to the SIR (1) model that takes into account the impacts of the spatial arrangement and population densities, as discussed in Section 2. The proposed model extends existing models examined by Lazo & De Cezaro (2021); Marques et al. (2022,2); Maurmann et al. (2023) and Kolokolnikov & Iron (2021) by integrating the concept of infection saturation discussed in Kolokolnikov & Iron (2021) into a model involving $n \geq 1$ interacting populations as proposed in Lazo & De Cezaro (2021); Marques et al. (2022,2); Maurmann et al. (2023). To our knowledge, no model involving n interacting populations with saturation has been previously proposed or examined in the literature. In Subsection 2.1, we will demonstrate the well-posedness of the proposed model, indicating that it possesses a unique solution that varies continuously based on the initial conditions and parameters. Section 3 will present various numerical simulations of the model, incorporating assumptions about the dynamics of a disease with multiple circulating strains. Finally, in Section 4, we will summarize the key findings and suggest potential avenues for future research.

2 AGENT-BASED SIR MODEL

To determine the model, we will assume that every person in the population i, where i ranges from 1 to n, acts as an agent. Each of these agents has a radius r_i, within which interactions occur between agents from compartments S_i and I_j in the same region. These interactions, which last an average time μ_{ij}, lead to the spread of infection with a probability p_{ij}.

Given the uniformity within each population (though not necessarily throughout the population), the probability of a susceptible individual from group i coming into contact with an infected individual from group j (where $i, j = 1, \cdots, n$) can be expressed as $a_{ij} = p_{ij} r_j^2 \pi / A_j$, with A_j representing the general area inhabited by population j.

The following lemma defines the model presented below as an agent-based mean field model, extending the findings in Kolokolnikov & Iron (2021) to n interacting populations.

Lemma 2.1. *Let r_j be significantly smaller compared to the size of A_j. Then the probability of an individual S_i getting infected by an infected agent I_j is determined by $\mu_{ij}(1-(1-a_{ij})^{I_j})$. Specifically, if $0 < a_{ij} << 1$, which occurs when $r_j << A_j$, then $\mu_{ij}(1-(1-a_{ij})^{I_j})$ is approximately equal to $\mu_{ij}(1-\exp(-a_{ij}I_j))$.*

Proof. Let E_{ij} represent the probability that an individual from S_i is located within a radius circle r_j of an individual from I_j. In such cases, the probability of transmission is determined by $p_{ij}E_{ij}$. It is important to note that E_{ij} denotes the proportion of the total area covered by the combined disks of I_j, where $j = 1, \cdots, n$. When r_j is small, E_{ij} is approximately equal to $a_{ij}I_j$. As the population within I_j grows, the circles start to overlap, causing E_{ij} to eventually reach a saturation point with a probability of 1.

Claim: $E_{ij} = a_{ij}^j$.

The claim is proved by employing induction in j while keeping $i \in \{1, \cdots, n\}$ fixed. When $j = 1$, E_{i1} represents the probability that an individual of S_i is within the disk of radius r_{i1}, with an area of $a_{i1} = \pi r_{i1}^2/A_j$. Therefore, $E_{i1} = a_{i1}$. Subsequently, E_{i2} denotes the anticipated area of overlap of two disks of radius r_{ij}, and so forth. Consequently, $E_{ij} = C(a_{ij})^j$. As $a_{ij} = 1$ leads to E_{ij} reaching a maximum value of 1, it follows that $c = 1$.

Thus, $E_{ij} = -\sum_{k=1} I_j C(I_j; k) a_{ik}^k = 1 - (1 - a_{ij})^{I_j}$, where $C(I_j; k)$ is the combination of the area of all circles of radius r_{ij}, without intersections. □

It follows from Lemma 2.1, that the agent-based multi-population SIR model, with vital dynamics is given by

$$\begin{aligned} S_i'(t) &= \Lambda_i - \sum_{j=1}^{n} \mu_{ij} \left(1 - exp(-a_{ij} I_j(t))\right) S_i(t) - m_i S_i(t)\,, \\ I_i'(t) &= \sum_{j=1}^{n} \mu_{ij} \left(1 - exp(-a_{ij} I_j(t))\right) S_i(t) - (\gamma_i + m_i) I_i(t)\,, \\ R_i'(t) &= \gamma_i I_i(t) - m_i R_i(t)\,. \end{aligned} \tag{4}$$

The model (4) will be examined with the initial conditions specified in (3).

It should be noted that the model (4) is an extension of the model examined in Kolokolnikov & Iron (2021) and Lazo & De Cezaro (2021); Marques et al. (2022,2); Maurmann et al. (2023) because it considers $n \geq 1$ interacting populations with saturation. Furthermore, the proof of Lemma 2.1 demonstrates that the model (4) is a generalization of a Reed-Frost model, as shown, for example, Abbey (1952); Mistro & Rodrigues (2021) and the related literature.

In the following, we state the relation between the saturated SIR model (4) to the SIR model without saturation 2.

Remark 2.1. *Suppose that the population affected, denoted as $I_j(t)$, is relatively low. By applying the Taylor approximation, it can be deduced that $1 - \exp(a_{ij}I_j(t)) \approx a_{ij}I_j(t)$. Consequently, the model* (4) *can be considered identical to the model 2 when $\beta_{ij} = \mu_{ij}a_{ij}$.*

2.1 Well-posedness

In the forthcoming discussion, we will demonstrate the well-posedness of the SIR model with saturation for multiple interacting populations (4), given the initial conditions (3). To accomplish this, we refer to $U(t) = (S_1(t), I_1(t), R_1(t), \cdots, S_n(t), I_n(t), R_n(t))^T$, a vector comprising $3n$ coordinates that represents a feasible solution for the model (4). Furthermore, we will denote $F(t, U(t))$ as the vector function that embodies the right-hand side of the model (4), with its components corresponding to the respective equations in the system (4).

The first result is a lemma that will help to demonstrate the main result.

Lemma 2.2. *Assuming that the model 4 satisfies the general assumptions, consider $N(t) = \sum_{i=1}^{n} N_i(t)$, where $N_i(t)$ represents the total population of individuals in group $i \in \{1, \cdots, n\}$. It is assumed that $m_i \geq \overline{M}$ for all $i \in \{1, \cdots, n\}$. Consequently, $N(t)$ is bounded uniformly.*

Proof. Summing up all the equation in model (4) results in

$$\dot{N}(t) = \sum_{i=1}^{n} \dot{N}_i(t) = \sum_{i=1}^{n} \Lambda_i - \sum_{i=1}^{n} m_i N_i(t)\,. \tag{5}$$

Let $\overline{\Lambda} = \max_{i\in\{1,\cdots,n\}} \Lambda_i$ and $\overline{M} = \min_{i\in\{1,\cdots,n\}} m_i$. Hence, we get

$$\dot{N}(t) = n\overline{\Lambda} - \overline{M}N(t)\,. \tag{6}$$

Therefore, the Gronwall inequality (see Techl (2012)) implies that

$$N(t) \leq n\frac{\overline{\Lambda}}{\overline{M}} + N(t=0)e^{-\overline{M}}\,. \tag{7}$$

□

Remark 2.2. *The assumption in Lemma 2.2 that $m_i \geq \overline{M}$, for every $i \in \{1, \cdots, n\}$, is not limiting. If $m_i = 0$ for some i, then according to the comparison principle Techl (2012), it can be deduced that the solution of model* (4) *with $m_i = 0$ is less than the solution with $m_i > 0$.*

Lemma 2.3. *Let $F(t,U(t))$ be defined as mentioned above. The Jacobian matrix of $F(t,U(t))$, denoted by $J(t,U(t))$, consists of all elements given by continuous functions in terms of t. Consequently, it is uniformly continuous in any interval $t \in [0,T]$, for any $T > 0$. Furthermore, there exists a positive constant L such that $J(t,U(t)) \leq L$. Additionally, there exist constants $C_1, C_2 \geq 0$ such that*

$$\|F(t,U(t))\| \leq C_1 + C_2\|U(t)\|\,. \tag{8}$$

Proof. The calculations for the first three rows of the Jacobian matrix $J(t,U(t))$ will be demonstrated, and the results for the remaining rows are similar.

Note that $\frac{\partial f_1(t,U(t))}{\partial S_j(t)} = -\mu_{11}\sum_{j=1}^{n}(1-exp(-a_{1j}I_j(t)))-m_j$ if $j=1$ and zero otherwise. Furthermore, $\frac{\partial f_1(t,U(t))}{\partial I_j(t)} = \mu_{11}a_{1j}S_1 exp(-a_{1j}I_j(t))$ and $\frac{\partial f_1(t,U(t))}{\partial R_j(t)} = 0$ for all $j = 1,\cdots,n$. Now, $\frac{\partial f_2(t,U(t))}{\partial S_j(t)} = -\frac{\partial f_1(t,U(t))}{\partial S_j(t)}$, $\frac{\partial f_2(t,U(t))}{\partial I_j(t)} = -\frac{\partial f_1(t,U(t))}{\partial I_j(t)} - \zeta_j$, where $\zeta_j = (\gamma_1 + m_1)$ for $j=1$ and zero otherwise. Finally, $\frac{\partial f_3(t,U(t))}{\partial I_1(t)} = \gamma_1$, $\frac{\partial f_3(t,U(t))}{\partial R_1(t)} = m_1$ and all other partial derivatives are null.

Due to the boundedness of $N(t)$ as stated in Lemma 2.2, it can be inferred that the lemma holds. □

The following statement serves as a supporting outcome for the subsequent Theorem.

Proposition 2.1. *The function $F(t,U(t))$ is continuous for t in the interval $[0,T]$ and is Lipschitz continuous with respect to $U(t)$ for any $T > 0$.*

Proof. From the definition of the model (4) that each row of $F(t,U(t))$ is composed of sums and products of continuous functions. Therefore, $F(t,U(t))$ is continuous with respect to $t \in [0,T]$. Furthermore, it follows from Lemma **??** that each coordinate of the Jacobian matrix $J(t,U(t))$ is composed of continuous functions in $[0,T]$.

Moreover, it follows form the Mean Value Theorem Sotomayor (1979) and Lemma 2.3 that there is $Z(t)$ between $U(t)$ and $\tilde{U}(t)$ such that

$$\|F(t,U(t)) - F(t,\tilde{U}(t))\| \leq \|J(t,Z(t))(t)\|\|U(t)-\tilde{U}(t)\| \leq L\|U(t)-\tilde{U}(t)\|$$

thus guaranteeing Lipschitz continuity of $F(t,U(t))$. □

Now we can prove the main theoretical result of this work.

Theorem 2.1. *Assume that the hypotheses of Proposition 2.1 are true. Then:*

i) There is a unique continuous solution $U(t)$ for the model (4)-(3)*, for all $t \in [0, T]$. This solution depends continuously on the initial conditions* (3) *and the model parameters* (4)*.*

ii) The solution $u(t)$ can be continuously extended to the non-negative real line.

Proof. It follows from Proposition 2.1 that $F(t, U(t))$ is continuous with respect to t and Lipschitz continues with respect to $U(t)$, for any $t \in [0, T]$. Therefore, it follows from Picard's Theorem and Gronwall's inequality Techl (2012) the existence of a continuous solution $U(t)$, as stated in the Theorem, item i). Furthermore, Lemma 2.3 guarantee the linear growth of $\|F(t, U(t))\|$ (see the inequality (8)). Therefore, it follows from (Techl, 2012, Theorem 2.17) that item-ii) is true. □

3 NUMERICAL SIMULATIONS

In this section, we will present the results of several numerical simulations of the model (4), considering the initial conditions (3), when dealing with two interacting populations ($n = 2$). The solutions were numerically approximated for the simulated scenarios using the fourth-order Runge-Kutta method Ascher & Greif (2011), on a uniform grid with a step size of $h = 10^{-2}$. The numerical solver is implemented in MATLAB, running on an Windows 10 operational system 64 bits. We chose the fourth-order Runge-Kutta since it is easy to implement and reduces the stiffness effect in the simulations. However, according to Silva et al. (2023), some implicit numerical scheme shall be used.

The simulations presented in the following are performed under the scenario where both populations are symmetric, each with a total population of $N_1 = N_2 = 500$. The interaction between these populations is reciprocal, denoted by $\mu_{12} = \mu_{21} = 0.01$. Furthermore, the recovery rate is assumed to be $\gamma_j = 0.05$ for both populations, while $\Lambda_i = \mu_i = 0.001$ is considered. The authors have deliberately selected these parameters in all simulations to reflect the implications of incorporating saturation into a multi-population model, drawing from the parameters derived in Kolokolnikov & Iron (2021).

3.1 The impacts where the diseases originated

Here, we discuss how the initial conditions influence the dynamics. Specifically, the simulations illustrate the consequences of the disease's point of origin and subsequent transmission.

SCENARIO 1: This scenario is represented in Figure 1 in which we present the scenario in which the disease begins in population 1 ($I_1(0) > 0$) while, at the beginning of the time, population 2 is free from the disease ($I_2(0) = 0$). In this way, the initial conditions are considered to be $S_1(0) = S_2(0) = 500$, $I_1(0) = 10$, $I_2(0) = 0$, $R_1(0) = R_2(0) = 0$. We will also assume that the radius $r_j = 0.1$, while $p_j = 0.5$, that is, each encounter has a 50% chance of infecting an individual. These parameters correspond to $a_j = 0.0157$, for $j = 1, 2$. In this case, the infected populations are denoted by $I_j(t)$, for $j = 1, 2$

Figure 1 – Dynamics of infected population in the scenarios presented in SCENARIO 1

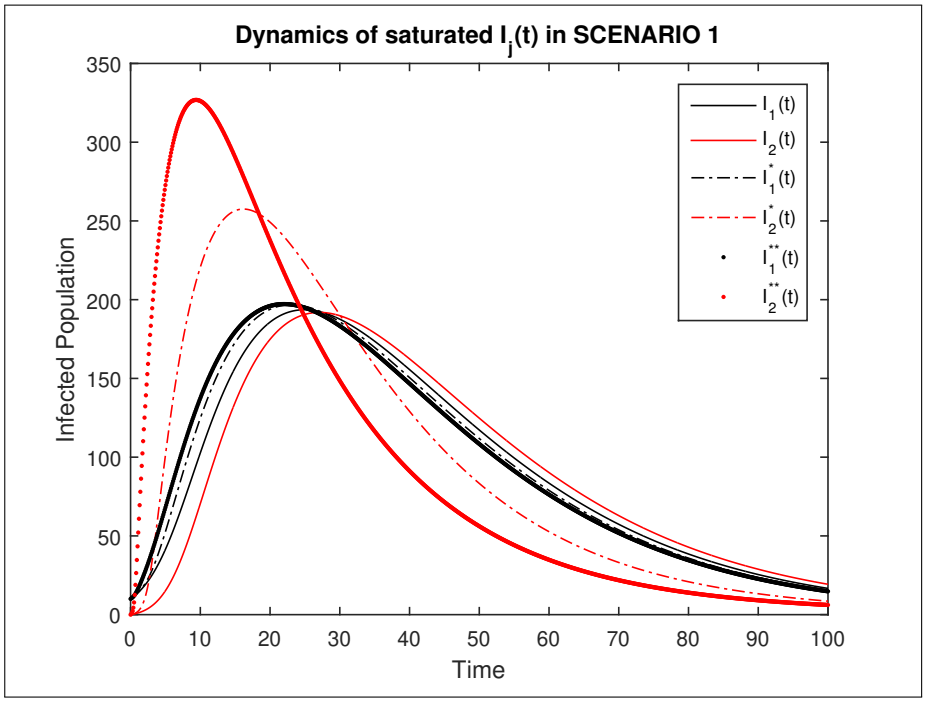

Source: the authors (2024)

Figure 1 also illustrates a scenario where the disease, after being transmitted from population 1 to population 2, mutates or undergoes another process that increases its transmissibility. This leads to $r_2^* = 2r_2$ and $\mu_{21}^* = 2\mu_{21}$, as well as $r_2^{**} = 4r_2$ and $\mu_{21}^{**} = 4\mu_{21}$. The other parameters remain constant as previously defined. In this case, the solution for the infected population is denoted by $I_j^*(t)$ and I_j^{**}, where $j = 1, 2$, respectively.

The findings illustrated in Figure 1 indicate that the mutation, which increases transmissibility, predominantly affects population 2, with the behavior of population 1 remaining largely unchanged.

SCENARIO 2: This situation is shown in Figure 2, where we illustrate a scenario in which the disease starts in population 2 ($I_2(0) > 0$), while population 1 is disease-free at the initial time ($I_1(0) = 0$). Initially, the conditions are set as $S_1(0) = S_2(0) = 500$, $I_1(0) = 0$, $I_2(0) = 10$, $R_1(0) = R_2(0) = 0$. The rest of the parameters and the simulated scenarios (including mutations) are the same as described in SCENARIO 1.

Figure 2 – Dynamics of infected population in the scenarios presented in SCENARIO 2

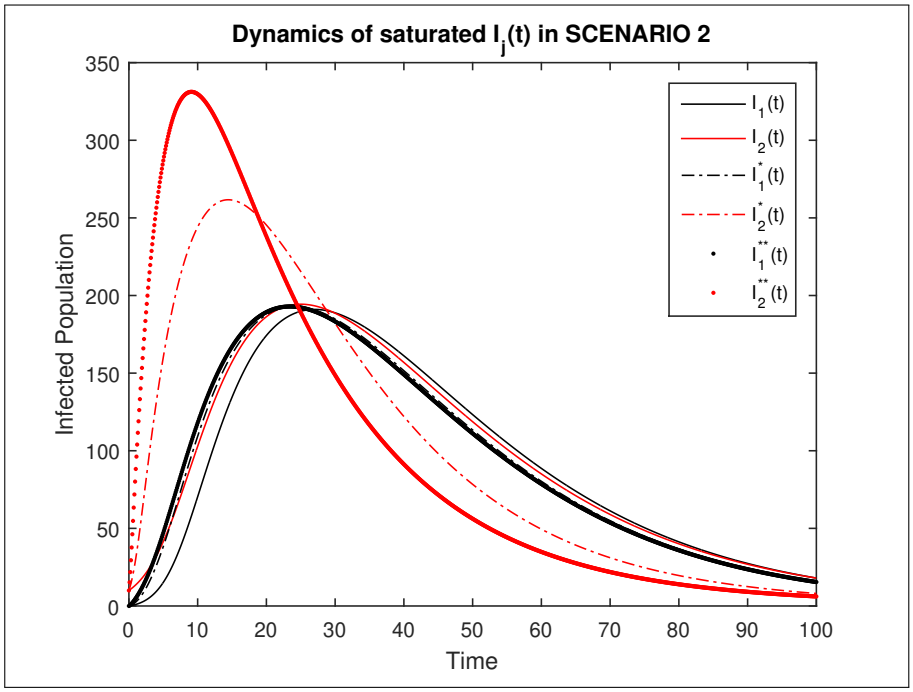

Source: the authors (2024)

The findings illustrated in Figure 2 indicate independently if the diseases starts in population 2, or in population 1 (compare with SCENARIO 1 presented in Figure 1) the mutation, which increases transmissibility, predominantly affects population 2, with the behavior of population 1 remaining largely unchanged. There is a diminute shift to the left in the dynamics of infection in simulated SCENARIO 2 compared to SCENARIO 1, mainly due to the initial conditions and the high infection rate in the population where the disease starts.

In light of the findings of SCENARIO 1 and 2, it can be inferred that the dynamic response of the infected population is not influenced by the initial conditions of the model (2).

3.2 Comparison between the dynamics of the SIR model with and without saturation

In this section, we provide a comparison of the dynamics in the simulation scenarios for the SIR model with saturation as specified in (4) and the SIR model without saturation as shown in (2).

SCENARIO 3: The situation illustrated in Figure 3 depicts the behavior of the group of people who are infected, considering the starting conditions and the factors specified in SCENARIO 1. This is based on the SIR model with saturation (4) and the SIR model without saturation, as shown in (2). The connection between the contagious rates between the models is detailed in Remark 2.1.

Figure 3 – Dynamics of infected population presented in SCENARIO 3. The notation $I_j(t)$ represents the dynamics for the infected population of the SIR model (4) with saturation, while the notation $w.s.I_j(t)$ represents the dynamics of the infected population for the SIR model (2) without saturation, for $j = 1, 2$, respectively

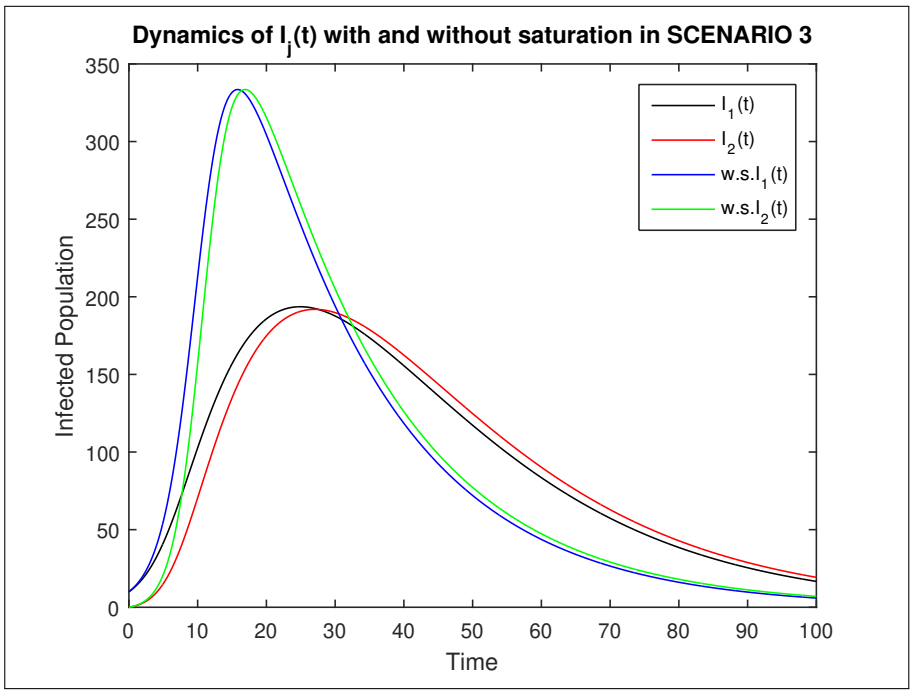

Source: the authors (2024)

Figure 3 illustrates that diseases spread more rapidly and affect a larger number of individuals at peak when the model without saturation (model (2)) is taken into account. On the other hand, the saturation in dynamics causes the infection in populations to take longer to vanish.

In Figure 4, we present the behavior of the infected populations in the scenarios with and without saturation in the dynamics. The comparison between those dynamics in the SIR model reveals that the saturation results in a milder disease dynamics when compared with the SIR model without saturation.

Figure 4 – Dynamics of infected population presented in SCENARIOS 1 to 3. The notation $I_j(t), I_j^*(t)$ and $I_j^{**}(t)$ represents the dynamics of the infected population of the SIR model (4) with saturation, while the notation $w.s.I_j(t), w.s.I_j^*(t)$ and $w.s.I_j^{**}(t)$ represents the dynamics of the infected population for the SIR model (2) without saturation, for $j = 1, 2$, respectively

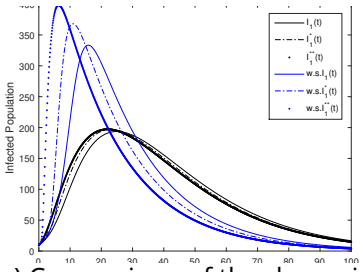

(a) Comparison of the dynamics for the infected population in population 1

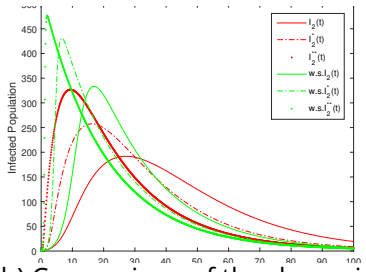

(b) Comparison of the dynamics of the infected population in population 2

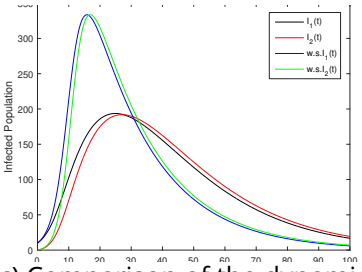

(c) Comparison of the dynamics of the infected population in the population without mutations in population 2

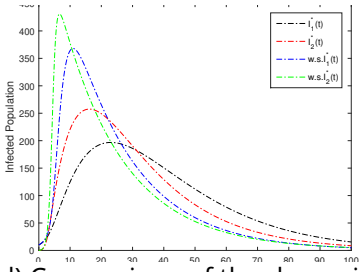

(d) Comparison of the dynamics for the infected population in the population with the mutation in population 2

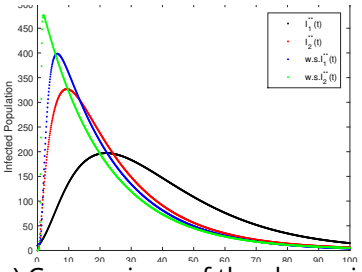

(e) Comparison of the dynamics of the infected population in the population with mutation in population 2. In this case, $r_2^* = 4r_2$ and $\mu_{21}^* = 4\mu_{21}$

Source: the authors (2024)

4 CONCLUSIONS

In this paper, we investigate the impact of epidemic spread in a model of SIR type with saturation among multiple interacting populations. The model proposed here is derived from an average threshold that considers multiple agents, extending the models examined in Kolokolnikov & Iron (2021) and Lazo & De Cezaro (2021); Marques et al. (2022,2); Maurmann et al. (2023). Theoretical analysis confirms the model's well-posedness. Additionally, we conduct numerical simulations for a scenario involving two interacting populations, where we also explore the scenario where the disease mutates upon transmission, leading to increased transmissibility. A comparison between the dynamics of the SIR model with and without saturation reveals that saturation results in a milder disease dynamics.

ACKNOWLEDGEMENTS

Lara Rocha thanks the support of CNPq under grant IC 11985 / 2023-9.

Adriano De Cezaro thanks the partial financial support of the National Council for Scientific and Technological Development - CNPq, and Fundação de Amparo à Pesquisa do Estado do Rio Grande do Sul - FAPERGS, under Grant 23/2551-0001824-1.

REFERENCES

Abbey, H. (1952). An examination of the reed-frost theory of epidemics. *Hum. Biol.*, *24*(3):201–233.

Allen, L. J. S. (2007). *An introduction to Mathematical Biology*. Pearson Prentice Hall.

Ascher, U. & Greif, C. (2011). *A First Course in Numerical Methods*. (1st ed). SIAM.

Dhaoui, I., Van Bortel, W., Arsevska, E., Hautefeuille, C., Alonso, S. T., & Kleef, E. (2022). Mathematical modelling of covid-19: a systematic review and quality assessment in the early epidemic response phase. *International Journal of Infectious Diseases*, *116*:S110.

Hethcote, H. W. (2000). The mathematics of infectious diseases. *SIAM Review*, *42*(4):599–653.

Kermack, W. & Mckendrick, A. (1927). A contribution to the mathematical theory of epidemics. *The Royal Socity*, *115*(772):700–721.

Kolokolnikov, T. & Iron, D. (2021). Law of mass action and saturation in sir model with application to coronavirus modelling. *Infectious Disease Modelling*, *6*(1):91–97.

Kutter, J. S., Spronken, M. I., Fraaij, P. L., Fouchier, R. A., & Herfst, S. (2018). Transmission routes of respiratory viruses among humans. *Current Opinion in Virology*, *28*:142–151.

Lazo, M. J. & De Cezaro, A. (2021). Why can we observe a plateau even in an out of control epidemic outbreak? a seir model with the interaction of n distinct populations for covid-19 in brazil. *Trends in Computational and Applied Mathematics*, 22(1):109–123.

Marques, J. C., De Cezaro, A., & Lazo, M. J. (2022). A sir model with spatially distributed multiple populations interactions for disease dissemination. *Trends in Computational and Applied Mathematics*, *23*(1):143–154.

Marques, J. C., De Cezaro, A., & Lazo, M. J. (2023). On an emerging plateau in a multi-population sir model. *preprint*, 23(1):1–21.

Maurmann, A. C., Travessini De Cezaro, F., & Cezaro, A. (2023). A fractional sirc model for the spread of diseases in two interacting populations. *Latin-American Journal of Computing*, *10*(2):46–57.

Mistro, D. C. & Rodrigues, L. A. D. (2021). Impacto do distanciamento social em um modelo discreto para covid-19. *Ciência e Natura*, *43*(Ed. Esp.):e12.

Silva, M. I., Marques, J. C., Conza, A. O., De Cezaro, A., & Gomes, A. C. F. N. (2023). The stiffness phenomena for the epidemiological sir model: a numerical approach. *Latin-American Journal of Computing*, *10*(2):32–45.

Sotomayor, J. (1979). *Lições de Equações Diferenciais Ordinárias*. (11th vol). Instituto de Matemática Pura e Aplicada, CNPq.

Techl, G. (2012). *Ordinary Differential Equations and Dynamical Systems*. (140th vol, Graduate Studies in Mathematics). AMS.

Author contributions

1 – Lara Beatriz Rocha Vieira (Corresponding Author)
Mathematician
https://orcid.org/0000-0001-8510-9424 • lararrocha4@gmail.com
Contribution: Conceptualization; Methodology; Writing – Original Draft Preparation

2 – Fabiana Travessini De Cezaro
Mathematician
https://orcid.org/0000-0001-9401-5315 • fabi.travessini@gmail.com
Contribution: Conceptualization; Methodology; Writing – Review

3 – Adriano De Cezaro
Mathematician
https://orcid.org/0000-0001-8431-9120 • decezaromtm@gmail.com
Contribution: Conceptualization; Methodology; Writing – Review

How to cite this article

Vieira, L. B. R., Travessini De Cezaro, F., & De Cezaro, A. (2024). On an agent-based SIR model for multi-populations. *Ciência e Natura*, Santa Maria, v. 47, spe. 1, e89848. DOI: https://doi.org/10.5902/2179460X89848.